Science of the Total Environment 912 (2024) 168898

Contents lists available at ScienceDirect

Science of the Total Environment

journal homepage: www.elsevier.com/locate/scitotenv

Evaluating the opportunities for mainstream P-recovery in anaerobic/anoxic/aerobic systems

Mengqi Cheng, Congcong Zhang, Albert Guisasola *, Juan Antonio Baeza

GENOCOV, Departament d'Enginyeria Química, Biològica i Ambiental, Escola d'Enginyeria, Universitat Autònoma de Barcelona, Bellaterra, Barcelona, Spain

HIGHLIGHTS

- Anaerobic reactor purging boosted PAO activity, raising P concentration by 27 %.
- Max P-recovery from supernatant could reach 51.6 % for anaerobic fermented WAS
- Low Mg^{2+} and NH_4^+ hinder the maximum struvite precipitation results
- Ca^{2+} concentration is key to have a high percentage of struvite in the precipitate

GRAPHICAL ABSTRACT

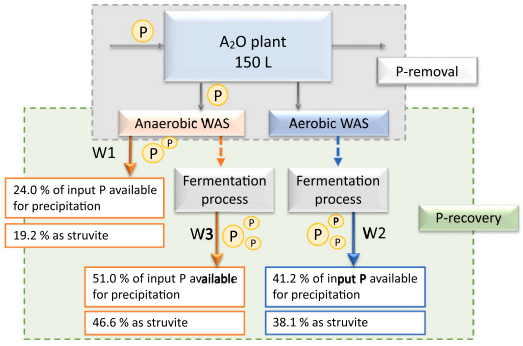

ARTICLE INFO

Guest Editor: Ignasi Rodriguez Roda

Keywords:
Chemical equilibrium model
Enhanced biological phosphorus removal (EBPR)
Nutrient removal
P recovery

ABSTRACT

Mainstream P-recovery can help wastewater treatment plants (WWTPs) to effectively maintain good enhanced biological phosphorus removal (EBPR) while helping to recover P. In this study, a pilot-scale anaerobic-anoxic-aerobic (A_2O) process was operated for simultaneous COD/N/P removal and P-recovery under different operational conditions. The operation with conventional extraction of waste activated sludge (WAS) from the aerobic reactor was compared to the mainstream P-recovery strategy of WAS extraction from the anaerobic reactor. Successful nutrient removal was obtained for both scenarios, but the anaerobic WAS extraction results improved polyphosphate accumulating organisms (PAOs) activity by increasing almost 27 % P concentration in the anaerobic reactor. WAS fermentation was also evaluated, showing that anaerobic WAS required only 3 days to reach a high P concentration, while the aerobic WAS fermentation required up to 7 days. The fermentation process increased the amount of soluble P available for precipitation from 24.4 % up to 51.6 % in the fermented anaerobic WAS scenario. Results obtained by precipitation modelling of these streams showed the limitations for struvite precipitation due to Ca^{2+} interference and Mg^{2+} and NH_4^+ as limiting species. The optimum precipitation scenario showed that P-recovery could reach up to 51 % of the input P, being 90 % struvite.

* Corresponding author.
E-mail addresses: mengqi.cheng@autonoma.cat (M. Cheng), Albert.Guisasola@uab.cat (A. Guisasola), JuanAntonio.Baeza@uab.cat (J.A. Baeza).

https://doi.org/10.1016/j.scitotenv.2023.168898
Received 31 August 2023; Received in revised form 22 November 2023; Accepted 24 November 2023
Available online 26 November 2023

1. Introduction

Phosphorus (P) is an essential nutrient for all life activities and together with carbon, hydrogen, oxygen, and nitrogen plays a vital role in the formation of DNA and energy supply. The current population growth and the subsequent growing need for food has increased the P requirements for agriculture and industry. Current P sources (mostly mined phosphate rock) are finite and heterogeneously distributed around the world. In fact, some researchers have estimated that P resources could be depleted in the next 50–100 years (Cornel and Schaum, 2009) and this could lead to severe geopolitical issues. These challenges have driven attention intensively on scientific and political levels for decades. The EU considers phosphate rock and phosphorus (P) among its twenty-seven critical raw materials of high importance and high supply risk to the EU economy (European Commission, 2017). Hence, P-recovery strategies are needed in the frame of the current circular economy scenario.

Decades ago, a main concern of environmental engineers in this field was to control P discharge by its chemical/biological removal from wastewater since a large amount of P was discharged into water bodies. Its over-enrichment, known as eutrophication, has had detrimental effects on aquatic ecosystems but also has caused an unnecessary resource waste (Egle et al., 2016). However, nowadays, the paradigm of wastewater treatment plants (WWTPs) has shifted to P-recovery in view of reducing the dependency on natural P. Thus, WWTPs are becoming a vital convergence point for both P removal and P-recovery, which is expected to meet 15–20 % of the global P demand (Bouzas et al., 2019; Venkiteshwaran et al., 2018). Although the initial P-recovery strategy was the direct land application of sludge as fertilizer, concerns about environmental and health risks due to the possible presence of heavy metals, micropollutants, pathogens or other chemical compounds have made this approach decreasingly accepted (Rey-Martínez et al., 2022). Thus, different alternative technologies including struvite precipitation, ion exchange, and membrane filtration have been proposed for P-recovery from flows containing P at all access point in WWTPs. These points include effluent, sewage sludge, sludge ash, dewatering liquor, and digester supernatant (Forrest et al., 2008; Sarria et al., 2022). These technologies provide different operability, costs, and potential uses of the recovered material (Zhang et al., 2022). The recovered P can then be used as a sustainable fertilizer or as a raw material to produce various P-based products like magnesium-ammonium-phosphate (MAP, also known as struvite), hydroxyapatite (HAP) or vivianite. For instance, recovering P as struvite from sewage by obtaining a highly concentrated P solution has been reported as an added value of biosolids treatment (Sena et al., 2021).

The anaerobic/anoxic/aerobic (A_2O) configuration is the most common one integrating enhanced biological phosphorus removal (EBPR) with biological carbon and nitrogen removal in WWTPs (Metcalf&Eddy et al., 2014). EBPR is based on the proliferation of polyphosphate accumulating organisms (PAO), which are able to accumulate large amounts of P as polyphosphate (poly-P) when subjected under alternating anaerobic/aerobic (or anoxic) conditions. In EBPR, the P concentration in the anaerobic reactor increases multiple times with respect to the influent concentration due to PAO activity, enabling mainstream P-recovery strategies (Zhang et al., 2022). As reported, the continuous investigations were operated in EBPR process with the integration of induced crystallization (Hermassi et al., 2015; Hutnik et al., 2011).

Previous works have proposed to move the waste of activated sludge (WAS) from the conventional external recycle or aerobic reactor to the anaerobic reactor to obtain biomass with high concentration of polyhydroxyalkanoates (Baeza et al., 2017; Larriba et al., 2020). This strategy also fits with the implementation of mainstream P-recovery, which has been reported in lab-scale SBR configurations due to the lower requirement for configuration and space and the flexibility of operation (Guisasola et al., 2019). Considering that the amount of P extraction is the most critical parameter for efficient P-recovery and that excessive P extraction may hinder the amount of P stored in the cell, evaluating the volume of the anaerobic WAS is important to achieve high P-recovery efficiency and avoid system failures. However, there is currently a clear knowledge gap in implementing mainstream P-recovery strategies and revealing how it affects the final P-removal.

In this study, the possibility of extracting the purge from the anaerobic reactor as a mainstream strategy to improve P-recovery has been evaluated in a 150 L A_2O pilot plant, comparing it with the conventional strategy of extracting the WAS after aerobic conditions and studying the effect that this change of operation has on the plant performance. A theoretical study was also carried out on the pH, Mg^{2+} and NH_4^+ addition requirements to recover the highest amount of phosphorus as struvite.

2. Materials and methods

2.1. Equipment and operation parameters

The A_2O configuration (Fig. 1) comprised three continuously stirred tank reactors (28 L anaerobic R1, 28 L anoxic R2 and 90 L aerobic R3) and a settler (50 L). The plant was monitored on-line with DO (HACH CRI6050), pH (HACH CRI5335) and temperature (Axiomatic Pt1000) probes connected to multimeters (HACH CRI-MM44). Data was acquired and stored through custom-made AddControl software (LabWindows CVI, National Instruments) (Baeza, 2022). The system was operated at room temperature (22 ± 2 °C). The flow between reactors, purge and recirculation was regulated by means of peristaltic pumps (Watson Marlow 520-FAM) timed by the AddControl software.

The biomass for inoculation was obtained from the municipal WWTP of Baix Llobregat (Barcelona). WAS was discharged from the anaerobic or aerobic reactor depending on the specific period at the flow rate required to maintain the desired SRT. The HRT in the A_2O plant was about 23 h considering only the reactors and 31 h also considering the settler.

The synthetic plant influent was made by diluting a concentrated solution with a tap water stream to a total flow rate of 147.5 L/d. The composition of the concentrated solution followed our previous study (Zhang et al., 2023) and is shown in Table S1. The influent COD concentration (COD_{INF}) was 516 mg/L (COD_{LOAD} = 76.1 gCOD/d) with a COD ratio of 3:3:3:1 of sodium propionate, acetic acid, sucrose and sodium glutamate. The phosphorus in the influent (P_{INF}) was 10 mg P-PO_4^{3-}/L (P_{LOAD} = 1.47 g/d), while the influent ammoniacal nitrogen (TAN_{INF}) was 38 mg N-NH_4^+/L (N_{LOAD} = 5.6 g/d).

2.2. Performance indices

In terms of the removal performance, absolute P_{REM}, N_{REM} and COD_{REM} (g/d) were calculated as Eqs. (1)–(3), where P_{EFF}, N_{EFF}, COD_{EFF} (g/L) stand for the corresponding concentrations of soluble phosphorus, nitrogen and COD in the effluent and Q_{EFF} (L/d) stands for the effluent flowrate.

$$P_{REM} = P_{LOAD} - P_{EFF} \cdot Q_{EFF} \quad (1)$$

$$N_{REM} = N_{LOAD} - N_{EFF} \cdot Q_{EFF} \quad (2)$$

$$COD_{REM} = COD_{LOAD} - COD_{EFF} \cdot Q_{EFF} \quad (3)$$

The fate of inlet TAN was N in the biomass (%), N in the effluent (%) and denitrified N (%), which were calculated as Eqs. (4)–(6).

$$N_{BIOMASS}\ (\%) = \frac{N_{EFFB} + N_{WASB}}{N_{LOAD}} \cdot 100\% \quad (4)$$

$$N_{LIQUID}\ (\%) = \frac{(N\text{-}NH_4^+ + N\text{-}NO_3^- + N\text{-}NO_2^-)_{EFF} \cdot (Q_{EFF} + Q_{WAS})}{N_{LOAD}} \cdot 100\% \quad (5)$$

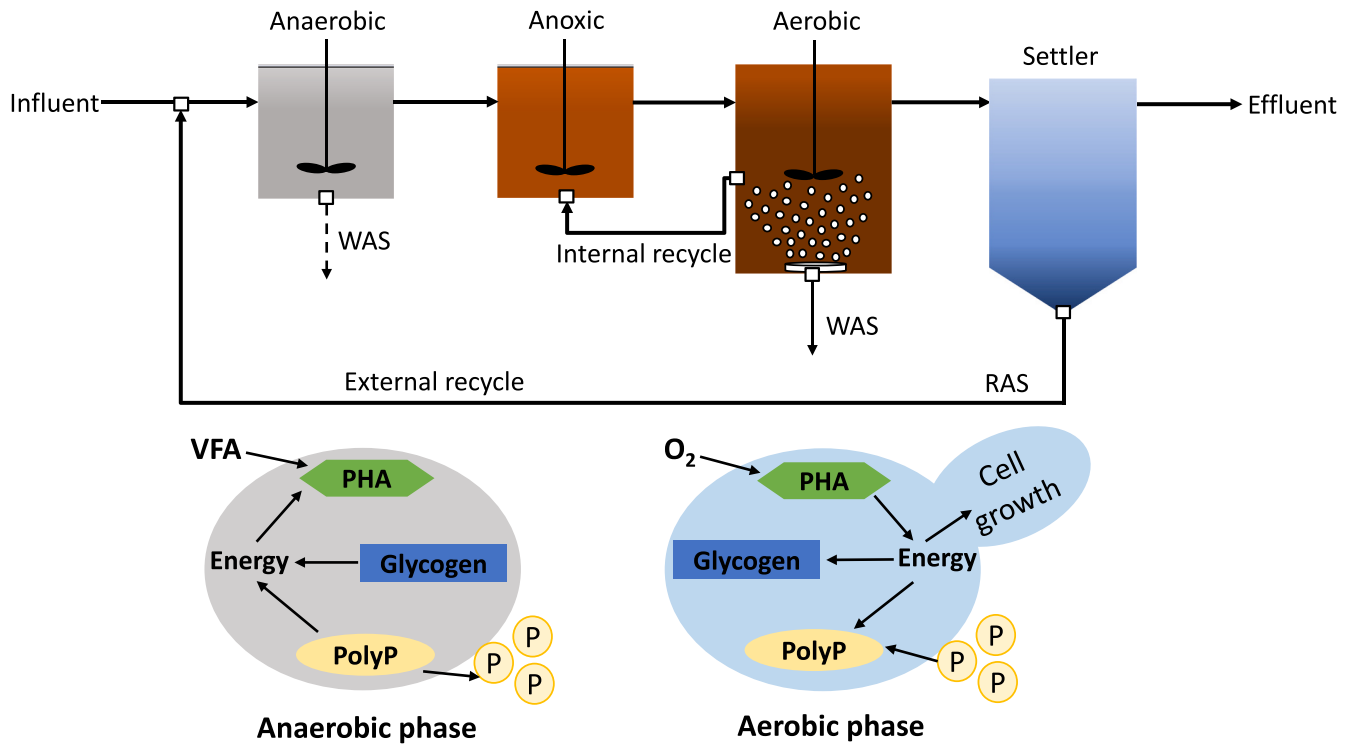

Fig. 1. Schematic diagram and general metabolism of PAOs in the A_2O system.

$$N_{DENITRIFIED}\ (\%) = 100 - N_{BIOMASS}\ (\%) - N_{LIQUID}\ (\%) \quad (6)$$

where N_{EFFB} (g/d) was the amount of nitrogen in the biomass of the effluent, N_{WASB} (g/d) the amount of nitrogen in the biomass of the WAS, $(N\text{-}NH_4^+ + N\text{-}NO_3^- + N\text{-}NO_2^-)_{EFF}$ (g/L) the total N concentration in the effluent and Q_{WAS} the flow rate of WAS. Note that the general formula for bacteria: $C_5H_7NO_2$ was assumed for the calculation of the percentage of N in the biomass from VSS measurements.

Similarly, the fate of COD_{LOAD} was COD in the biomass (%), in the effluent (%) and mineralized COD (%), which were calculated according to Eqs. (7)–(9).

$$COD_{BIOMASS}\ (\%) = \frac{COD_{EFFB} + COD_{WASB}}{COD_{LOAD}} \cdot 100\% \quad (7)$$

$$COD_{EFF}\ (\%) = \frac{COD_{EFF} \cdot Q_{EFF}}{COD_{LOAD}} \cdot 100\% \quad (8)$$

$$COD_{MINERALIZED}(\%) = 100 - COD_{BIOMASS}(\%) - COD_{EFF}(\%) \quad (9)$$

where COD_{EFFB} (g/d) was the amount of COD in the effluent biomass and COD_{WASB} the amount of COD in the biomass from the WAS. The COD from biomass was calculated from VSS measurements assuming the general formula for bacteria: $C_5H_7NO_2$, i.e. 1.416 gCOD/gVSS.

In order to estimate the maximum potential P-recovery from anaerobic supernatant and from fermented WAS, the P-recovery efficiency (PRE) was calculated assuming the ideal scenario that all the soluble P could be recovered, shown as Eq. (10), where the $P_{SUPERNATANT}$ (g/L) referred to the concentration of soluble P in the supernatant of the anaerobic reactor or of the fermented WAS, and Q_{WAS} (L/d) was the WAS flow rate extracted.

$$PRE(\%) = \frac{P_{SUPERNATANT} \cdot Q_{WAS}}{P_{LOAD}} \cdot 100\% \quad (10)$$

2.3. Chemical analysis

Liquid samples for concentration analysis of soluble phosphate, COD, ammonium, nitrate and nitrite were withdrawn from the three reactors almost daily. After the filtration with 0.22 μm filters (Millipore), phosphate was analysed by a phosphate analyser (115 VAC PHOSPHAX sc, Hach-Lange), ammonium concentration by an ammonia analyser (AMTAX sc, Hach-Lange), and nitrate and nitrite were detected with Ionic Chromatography (DIONEX ICS-2000). COD was measured by kits (LCK 314, 714, Hach) and a spectrophotometer (DR3900, Hach-Lange). Sludge samples were withdrawn from the reactors and effluent for the analysis of mixed liquor volatile suspended solids (VSS) and total suspended solids (TSS) by a heating oven (UF75, Memmert) and a high temperature muffle furnace (12/PR300, Hobersal). The sludge volume index (SVI) was calculated as volume (mL) of sludge from the aerobic reactor after settling for 30 mins over the TSS (g/L) measured on the same day.

2.4. Batch tests for anaerobic sludge fermentation

Two anaerobic batch tests of sludge fermentation were performed to investigate the evolution of $P\text{-}PO_4^{3-}$, $N\text{-}NH_4^+$, and Mg^{2+} profiles when biomass decays under anaerobic conditions. The experiments were conducted with biomass obtained from the aerobic and anaerobic WAS when the system was at pseudo steady state conditions during period I (day 17) and period III (day 50). A 1 L crystal brown bottle was filled with biomass and sparged with nitrogen gas to ensure anaerobic conditions. The bottle was maintained at room temperature, mixed daily, and liquid samples were taken to analyse until all biomass decayed nearly. pH was routinely monitored during the batch tests and it was maintained in the range of 7.35 and 7.85. No extra biomass was added during the whole period.

2.5. Simulation method

The chemical equilibrium model used in the present study was Visual MINTEQ (Ver 3.1), which supports the calculation of metal speciation, solubility equilibria, sorption etc. for different waters (Gustafsson, 2005). The experimental data of P-PO_4^{3-}, N-NH_4^+, and Mg^{2+} obtained from the anaerobic supernatant and sludge fermentation batch tests was used. All possible precipitation species suggested by MINTEQ were selected to establish the chemical equilibrium model. Different reaction conditions for different concentrations of P-PO_4^{3-}, N-NH_4^+, Mg^{2+}, Ca^{2+} and pH were simulated to estimate the possibilities of P-recovery.

The possible precipitation species in this N-P-Mg-Ca system included struvite ($MgNH_4PO_4{\cdot}6H_2O$), brucite ($Mg(OH)_2$), newberyite ($MgHPO_4{\cdot}3H_2O$), periclase (MgO) and $Mg_3(PO_4)_2$, hydroxyapatite (HAP, $Ca_5(PO_4)_3(OH)$), lime (CaO), brushite ($CaHPO_4{\cdot}2H_2O$), whitlockite (TCP, $Ca_3(PO_4)_2$) and monetite (DCP, $CaHPO_4$). However, only four species (struvite, $MgHPO_4{\cdot}3H_2O$, $Mg_3(PO_4)_2$ and HAP) were the final precipitated products based on the Visual MINTEQ results. This study set 156 different concentration scenarios for each phase based on the presence of Ca^{2+} (20–40-60 mg/L), pH (7.8–10.2) and N-NH_4^+ (batch result-50-75-100 mg/L) as shown in Table S2.

This modelling-based study assumes that the precipitator to be implemented in the WWTP will allow the equilibrium compositions to be achieved. Therefore, the model outputs represent the maximum theoretical yield of compounds that could be obtained in an optimally operated reactor at the setpoint pH. Thus, the performance observed in a full-scale system may be lower as it may be limited by the kinetics of the precipitation reactions. In fact, predicting/understanding the kinetics for struvite crystallization under the operational conditions of a WWTP (Elduayen-Echave et al., 2019) is an understudied topic that requires more consistent results to develop a functional predictive kinetic model (Natividad-Marin et al., 2023).

3. Results and discussion

3.1. A_2O system performance

The pilot plant was initially operated under an A_2O configuration implementing different WAS extraction strategies to evaluate its P-removal performance and the possible P-recovery (Table 1). The purge location was changed from conventional aerobic WAS (Period I) to anaerobic WAS (Period II) at 5 L/d. In the first case, most P was present as internal poly-P whereas, in the second case, an important fraction of P was dissolved in the liquid phase. Then, the WAS flow rate was increased to 7 L/d (anaerobic reactor) on day 42 (period III) to evaluate whether P-recovery could be increased without affecting P-removal performance. Figs. 2 and 3 show the evolution of P-PO_4^{3-}, N-NH_4^+, COD and solids under the different operation stages, whereas Tables 2 and 3 display the mass balances of P-PO_4^{3-}, N-NH_4^+ and COD and the evolution of solids during all the operational periods.

Period I was operated under conventional aerobic WAS (5 L/d and SRT around 20.6 ± 1.0 days) and it showed good P removal (absolute P_{REM} was 1.38 ± 0.01 g/d and P_{EFF} was 0.1 ± 0.1 mg/L), full nitrification, and almost full COD removal. Solids in the reactor were stable at 2.37 ± 0.10 g VSS/L and SVI was 332 ± 94 mL/g showing reasonable settleability for the pilot plant. The WAS location was then moved to the anaerobic reactor (5 L/d) in period II. Full ammonium, COD and P

Table 1
Operational conditions for each period under A_2O configuration.

Period	Days of operation	WAS extraction	WAS flow rate (L/d)
Start-up	1–4	Aerobic	0 to 5
I	5–20	Aerobic	5
II	21–41	Anaerobic	5
III	42–54	Anaerobic	7

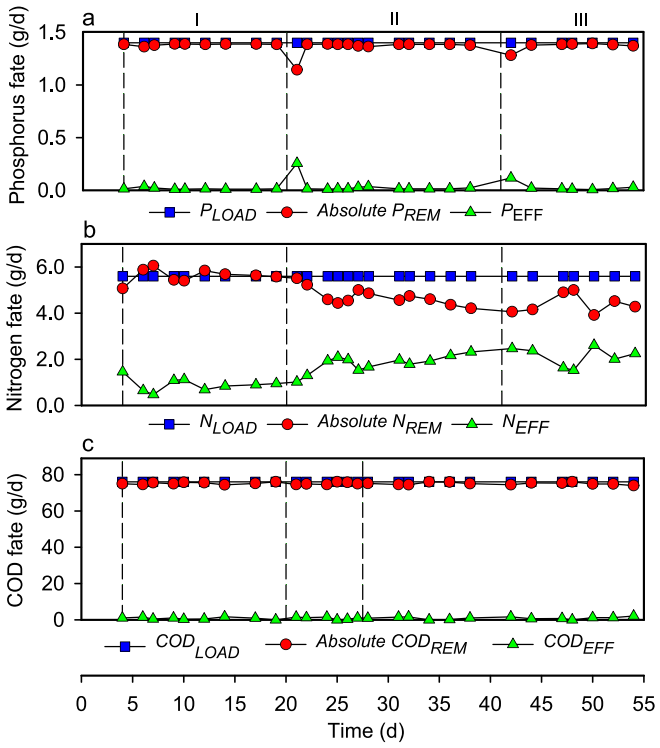

Fig. 2. Evolution of phosphorus (a), nitrogen (b) and COD (c) in different operation stages.

removal was observed on day 23 (P_{EFF} = 0.1 mg P/L) while anaerobic P (P_{ANA}) increased from 44 mg P/L to almost 56 mg P/L indicating an enhancement of PAO activity. However, N-NO_{3EFF}^- increased from 4.8 to 10.4 mg N/L leading to higher nitrate load to the anaerobic reactor (from 0.72 ± 0.19 to 1.55 ± 0.32 g/d) and lower percentual absolute N_{REM} (87 % to 72 %). This decrease in nitrate removal performance could be related to the fraction of COD lost when using anaerobic WAS extraction, not only related to the soluble COD that is not consumed in the anaerobic reactor, but also to the sludge containing a fraction of PHA that could be used for PAO denitrification in the anoxic reactor. It was estimated that about 2 % of COD load could be lost when using 5 L/d of anaerobic WAS extraction. Regarding the possible nitrite that could appear during nitrification and denitrification, it was not detected at any time during the operation. The VSS concentrations in the reactor and in the effluent when operating with the anaerobic WAS extraction were about 2.1 and 0.03 g/L, while SVI was 221 ± 12 mL/g, which did not lead to any settleability issues. As a conclusion, moving the WAS extraction from the aerobic to the anaerobic reactor improved PAO activity without affecting the P-removal performance but slightly decreasing the N-removal.

The anaerobic WAS flow was increased to 7 L/d on day 42 (period III) to increase the amount of potential mainstream P-recovery. Previous works showed that the higher the anaerobic purge, the higher the P-recovery opportunities but up to a certain threshold value (Zhang et al., 2022). Values higher than this threshold would lead to PAO activity deterioration. However, successful P-removal was maintained (P_{EFF} = 0.2 mg P /L) during period III, whereas P_{REM} was equal to those in periods I and II (1.44 vs 1.44 and 1.46 g P/d). Full nitrification and COD removal efficiency were still obtained. COD_{REM} was similar to the other two periods (75.3 vs 75.2 and 75.0 g/d), the fraction of COD in the liquid maintained the same (1 ± 1 %) while a slightly high fraction of COD in the WAS (34 ± 1 %) was observed (Table 2). Meanwhile, no ammonium was detected in the effluent. The percentage N_{REM} decreased to 67 % since the concentration N-NO_{3EFF}^- increased to 12.4 ± 2.4 mg/L, causing discharges in the effluent of 1.82 ± 0.36 g N/d. However, the sludge

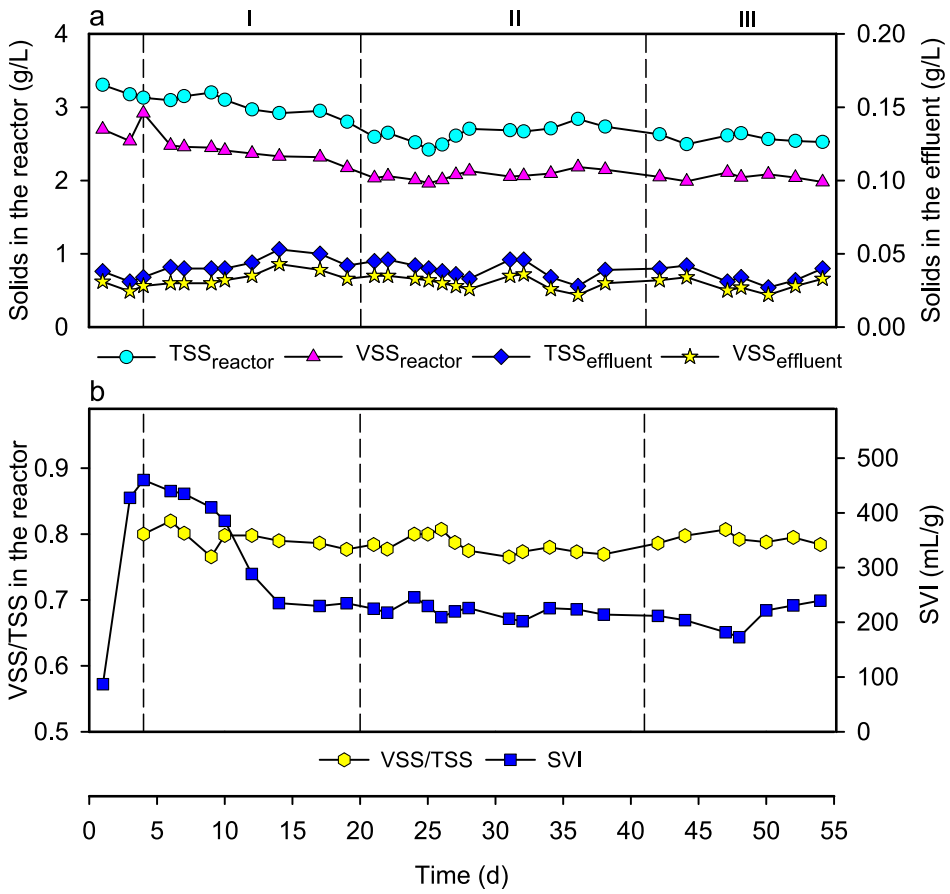

Fig. 3. Solids concentration in the reactor, effluent (a), the ratio of VSS/TSS in the reactor and SVI (b) of the solids in different operation stages.

Table 2
Mass balances and EBPR performance for each experimental period.

Period	Index	LOAD (g/d)	EFF (mg/L)	EFF (g/d)	REM (g/d)	Removal efficiency (%)	In the liquid (%)	In the WAS (%)	Additional (%)
I	P	1.47 ± 0	0.1 ± 0.1	0.02 ± 0.01	1.46 ± 0.01	98.9 ± 0.6	1 ± 1	99 ± 1	NA
	N	5.60 ± 0 [a]	4.8 ± 1.3 [b]	0.72 ± 0.19	4.88 ± 0.18	87.3 ± 3.2	13 ± 3	37 ± 1	50 ± 4 [c]
	COD	76.1 ± 0	22.2 ± 2.3	0.8 ± 0.6	75.3 ± 3.7	98.9 ± 0.7	1 ± 1	31 ± 1	68 ± 2 [d]
II	P	1.47 ± 0	0.3 ± 0.2	0.04 ± 0.03	1.44 ± 0.07	97.4 ± 4.6	3 ± 2	97 ± 1	NA
	N	5.60 ± 0 [a]	10.4 ± 2.2 [b]	1.55 ± 0.32	4.07 ± 0.32	72.7 ± 5.8	28 ± 6	33 ± 1	40 ± 5 [c]
	COD	76.1 ± 0	34.7 ± 3.1	0.9 ± 0.6	75.2 ± 4.2	98.8 ± 0.8	1 ± 1	28 ± 1	71 ± 2 [d]
III	P	1.47 ± 0	0.2 ± 0.3	0.03 ± 0.04	1.44 ± 0.04	97.8 ± 2.6	2 ± 1	98 ± 2	NA
	N	5.60 ± 0 [a]	12.4 ± 2.4 [b]	1.82 ± 0.36	3.78 ± 0.36	67.5 ± 6.4	33 ± 6	41 ± 1	27 ± 7 [c]
	COD	76.1 ± 0	27.9 ± 1.3	1.1 ± 0.7	75.0 ± 4.6	98.6 ± 0.9	1 ± 1	34 ± 1	64 ± 1 [d]

NA: not applicable.
[a] As N-NH_4^+.
[b] As N-NO_3^-.
[c] Denitrified N.
[d] Mineralized COD.

settleability was unaffected (SVI was 209 ± 25 mL/g). The ratio of VSS/TSS was about 0.79 (Table 3) which indicated a good PAO proportion in the sludge (Broughton et al., 2008). In summary, taking WAS from the anaerobic reactor could enhance P circularity by mainstream P-recovery in A_2O system, by selecting a proper WAS flowrate, although some decrease in denitrification could also be expected depending on the COD availability in the influent. Additional research under different influent COD concentration is required to assess the repeatability and significance of the decrease in denitrification performance depending on the specific scenario.

3.2. Evaluating maximum P-recovery at different WAS extraction locations

This section discusses the opportunities for mainstream P-recovery in an A_2O plant as a function of the WAS location. The first step for P-recovery is to obtain a stream with the highest concentration to facilitate a possible subsequent precipitation step. The extraction of WAS from the anaerobic reactor opens the possibility for mainstream P-recovery, as opposed to aerobic WAS extraction, where the concentration in the supernatant is very low (P_{AER} < 1 mg P/L) since the P is stored as intracellular poly-P. However, if the extracted sludge is subjected to a simple fermentation process, significant amounts of P can be released and thus increase its concentration to make recovery by precipitation possible.

Table 3
Average solids concentrations, VSS/TSS and settleability for each period.

Period	SRT (d)	VSS_{WAS} (g/L)	VSS_{EFF} (g/L)	TSS_{WAS} (g/L)	TSS_{EFF} (g/L)	VSS/TSS	SVI (mL/g VSS)
I	20.6 ± 1.0	2.37 ± 0.10	0.034 ± 0.005	3.02 ± 0.13	0.044 ± 0.005	0.792 ± 0.016	332 ± 94
II	20.5 ± 1.1	2.07 ± 0.06	0.031 ± 0.004	2.64 ± 0.12	0.039 ± 0.006	0.783 ± 0.013	221 ± 12
III	16.3 ± 0.6	2.04 ± 0.05	0.029 ± 0.004	2.57 ± 0.06	0.035 ± 0.006	0.793 ± 0.008	209 ± 25

This process is clearly to be applied to aerobic sludge, but it also allows to improve P release from anaerobic sludge. Then, it is worth discussing a first scenario using anaerobic WAS without fermentation (W1) and two scenarios with fermentation of aerobic WAS (W2) and anaerobic WAS (W3). In all three cases it is ideally assumed that the biomass in this stream can be perfectly separated and therefore for the numerical evaluation it is assumed that a supernatant of the same total volume as the WAS is left but without biomass. In this section the amount of soluble P that can be contained in these supernatants is evaluated, while in the following section the possible limitations for recovery due to the specific composition of the stream are studied by chemical precipitation simulation.

For the case W1 of anaerobic WAS without fermentation, P_{ANA} and the WAS flowrate were 55.9 ± 14.5 mg P/L and 5 L/d in Period II whereas the values were 51.4 ± 4.8 mg P/L and 7 L/d in period III. Then, 0.28 and 0.36 g P/d of those could be recovered from the anaerobic supernatant by mainstream P-recovery, respectively. Considering a constant P load of 1.47 g/d to the plant, about 19 % and 24 % of the input P was contained in this supernatant in periods II and III. Thus, increasing anaerobic purge from 5 to 7 L/d improved the maximum P-recovery by 5 %, while P_{ANA} increased the P_{INF} (10 mg/L) >5 times, which triggers the possibility of P-recovery by precipitation.

For cases W2 and W3, Fig. 4 shows the results of anaerobic fermentation tests conducted to understand the extent of PO_4^{3-}, NH_4^+ and Mg^{2+} release when the aerobic and anaerobic WAS were fermented. The time needed to reach a high *P* value was 7 and 3 days for aerobic (W2) and anaerobic WAS (W3), respectively. Afterwards, the experimental profiles were considered mostly stable. For case W2 of aerobic WAS after fermentation, P increased from 7.4 to 113.1 mg/L in the liquid phase, while the $N\text{-}NH_4^+$ and Mg^{2+} increased from 0 and 14.8 mg/L to 13.7 and 32.1 mg/L, respectively. Regarding case W3 with anaerobic WAS, P increased in only 3 days from 47.1 to 93.1 mg/L and $N\text{-}NH_4^+$ and Mg^{2+} increased from 16.1 and 26.7 mg/L to 40.3 and 22.1 mg/L, respectively. Consequently, the anaerobic WAS fermentation allowed a very high P concentration to be reached in 57 % less time, although the maximum concentration obtained for that time was 17 % lower. This difference would imply that for the design of the fermentation reactor, anaerobic WAS treatment could be considered to require approximately half the volume needed for aerobic WAS treatment.

WAS fermentation was useful to increase the fraction of P in the input that was ultimately dissolved in the supernatant and could eventually be recovered. Considering the last P concentrations of the fermentation batch tests and the WAS flow rates in each case, the fraction of P that could be recovered in the supernatant increased from 24.4 % in W1 to 41.7 % for W2 and to 51.6 % for W3 (Table 4), due to the higher anaerobic WAS flow rate (7 vs. 5 L/d) and despite the lower final concentration (108.8 mg P/L in W3 vs. 123.2 mg P/L in W2). In any case, based on the P mass balances in the plant, with P-removal higher than 97 %, and a steady state operation, the WAS stream must contain the total amount of P removed. Thus, there was still an important fraction of P accumulated as poly-P in the biomass and the operating conditions/duration of the fermentation process would need to be optimized to increase the amount of soluble P in the supernatant.

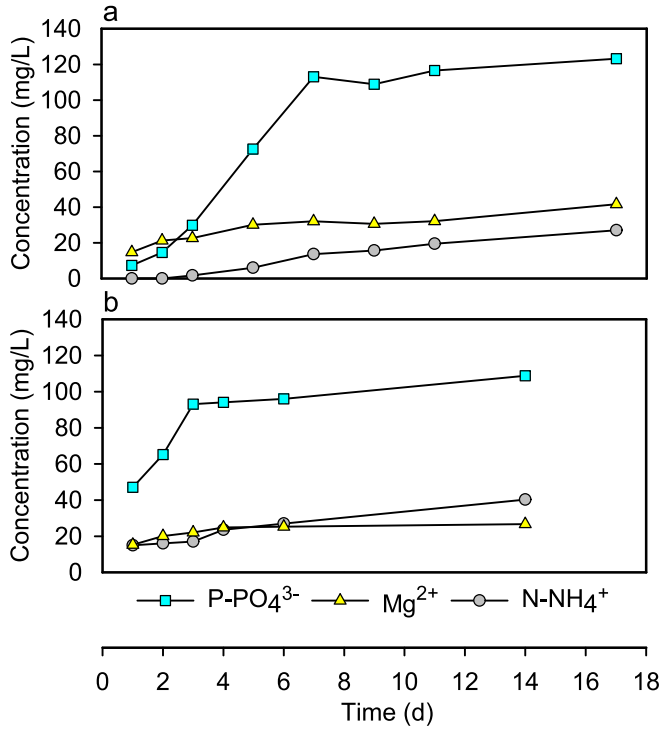

Fig. 4. Evolution of concentrations for $P\text{-}PO_4^{3-}$, $N\text{-}NH_4^+$ and Mg^{2+} during fermentation of WAS. a) W2 - aerobic WAS (5 L/d) and b) W3 - anaerobic WAS (7 L/d).

3.3. Identification of composition limitations for P-recovery using visual MINTEQ

The final values of $P\text{-}PO_4^{3-}$, $N\text{-}NH_4^+$ and Mg^{2+} from the three scenarios W1, W2 and W3 were used to simulate potential P-recovery options (preferably as struvite and HAP) under different conditions. of pH (from 7.8 to 12) and three different Ca^{2+} (20, 40 and 60 mg/L) concentrations (Fig. 5 and Fig. S1). Calcium was also considered for this study, as there is a high variability in its concentration depending on the wastewater and it is a species that can strongly influence the final composition of the precipitate.

Under these conditions where a possible calcium concentration is fixed and only the pH is varied, the three scenarios were not very favourable for precipitation. Most of $P\text{-}PO_4^{3-}$ remained dissolved, all calcium was precipitated as HAP and low struvite production was predicted as the streams were limited by Mg^{2+} or $N\text{-}NH_4^+$ concentration.

Table 4
Overall P-recovery efficiency from the supernatant of each scenario.

	W1	W2	W3
P_{Load} (g/d)	1.47	1.47	1.47
Maximum P-recovery from supernatant (g/d)	0.360	0.616	0.762
Maximum P-recovery from supernatant (%)	24.4	41.7	51.6
Maximum P precipitation efficiency by Visual Minteq (%)	98.5	98.8	98.8
Maximum theoretical precipitated P as struvite by Visual Minteq (%)	78.9	91.2	90.3
Maximum P-recovery as precipitate (%)	24.0	41.2	51.0
Maximum P-recovery as struvite (%)	19.2	38.1	46.6

*W1: anaerobic WAS without fermentation (7 L/d); W2: fermented aerobic WAS (5 L/d); W3: fermented anaerobic WAS (7 L/d).

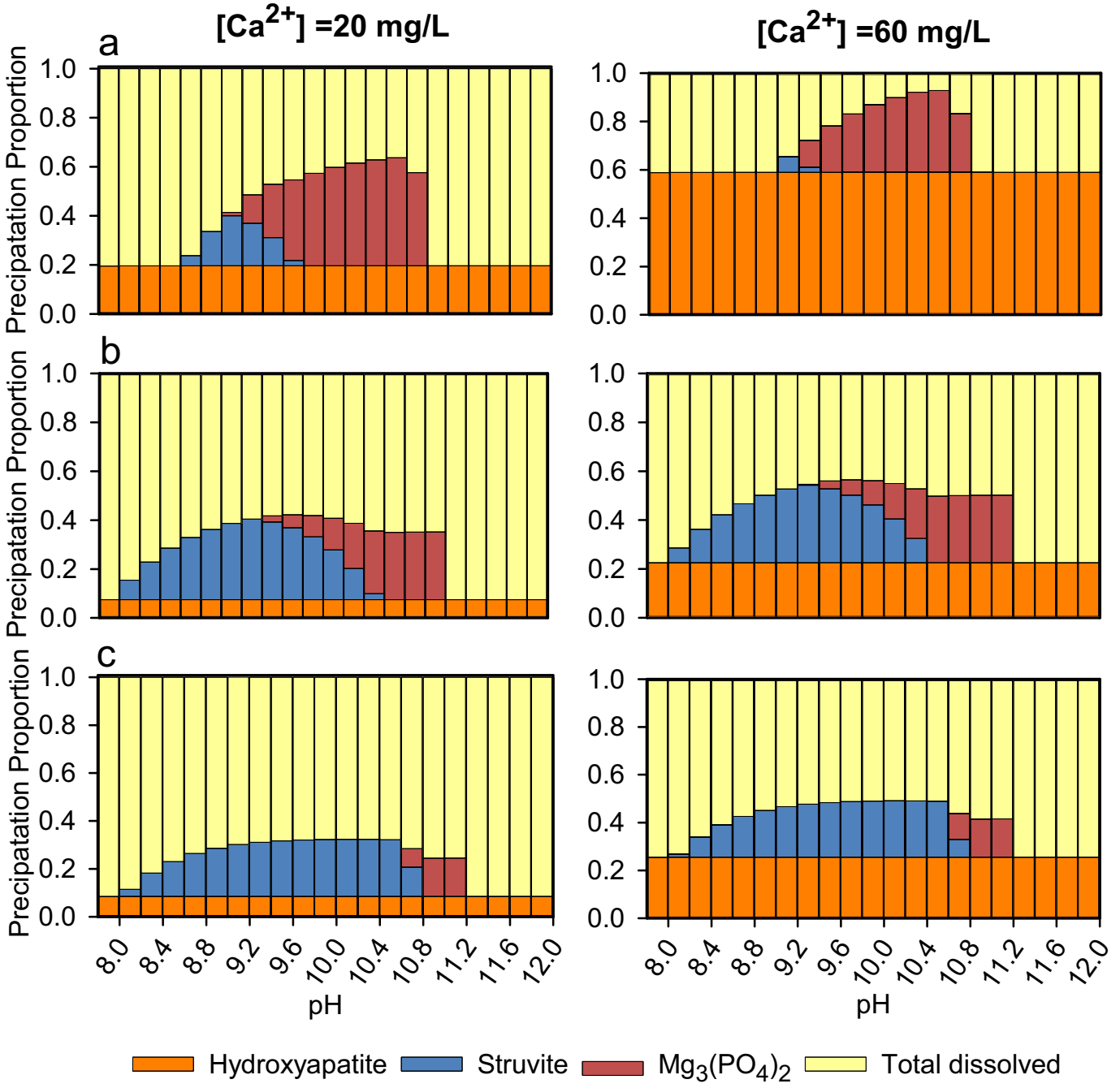

Fig. 5. Proportion of P-PO_4^{3-} in different precipitates as function of the pH range and Ca^{2+} concentration (20 and 60 mg/L) for a: W1 - anaerobic WAS (7 L/d), b: W2 - fermented aerobic WAS (5 L/d) and c: W3 - fermented anaerobic WAS (7 L/d).

Struvite precipitation shows a strict pH range (neither too alkaline nor too acidic improves the precipitation process) while HAP can be precipitated at all pH range.

The simulation results suggest that Ca^{2+} concentration limits the P-recovery as struvite as the first option for P precipitation is HAP as already reported (Lee et al., 2013). HAP precipitation cannot be considered as a bad situation since HAP can be valorised as a fertilizer for agriculture (Annisa et al., 2021; Zhang et al., 2022). The amount of HAP is proportional to the Ca^{2+} present, independently of P concentration and pH, as it is thermodynamically highly favoured. Ca^{2+} competes with Mg^{2+} and is therefore a key factor to consider when specifically targeting P-recovery as struvite (Li et al., 2016). The reported sequence for calcium-containing precipitations shows that the most unstable amorphous calcium phosphate (ACP) would appear first, and they would gradually transform to octacalcium phosphate (OCP) at pH of 7–9, then end transforming as HAP (Shih and Yan, 2016). Note that Visual MINTEQ does not account for kinetics and only shows the final steady-state and therefore the final precipitation form is HAP.

The simulation results for W1 case, anaerobic WAS before fermentation, show that the pH range for struvite precipitation depended on the amount of Ca^{2+} (Fig. 5a). For low Ca^{2+} concentrations (20 mg/L), struvite could be precipitated from pH = 8.6 to 9.6 with pH = 9 as optimal (about 20 % of P-PO_4^{3-} precipitated as struvite). The pH range was narrowed to 8.8–9.6 with the condition of 40 mg Ca^{2+}/L (as shown in Fig. S1), suggesting a higher Mg^{2+} amount was needed. The highest amount of precipitation also occurred at pH = 9 but with a lower

percentage of P-PO_4^{3-} precipitated as struvite: slightly above 14 %. Finally, the pH range was severely reduced at 60 mg Ca^{2+}/L to 9–9.2 due to the competition of Ca^{2+}. Again, pH = 9 was the optimal value with a much lower percentage of 6.4 % P-PO_4^{3-} precipitated as struvite while almost 59 % P-PO_4^{3-} precipitated as HAP. For the aerobic WAS results W2 (Fig. 5b), the pH range of struvite precipitation was 8 to 10.4, with an optimum around 32 % of total P-PO_4^{3-} at pH = 9.2 in all three Ca^{2+} concentration scenarios. The detailed data for all the scenarios are shown in Table 5. pH values higher than 9.2 resulted in competition between struvite and $Mg_3(PO_4)_2$.

When dealing with anaerobic WAS, the P-recovery efficiency was enhanced with the fermentation process (W3) by widening the pH range of struvite precipitation into 8 to 10.6, which can be attributed to the higher N-NH_4^+ concentration (Fig. 5c). However, the maximum

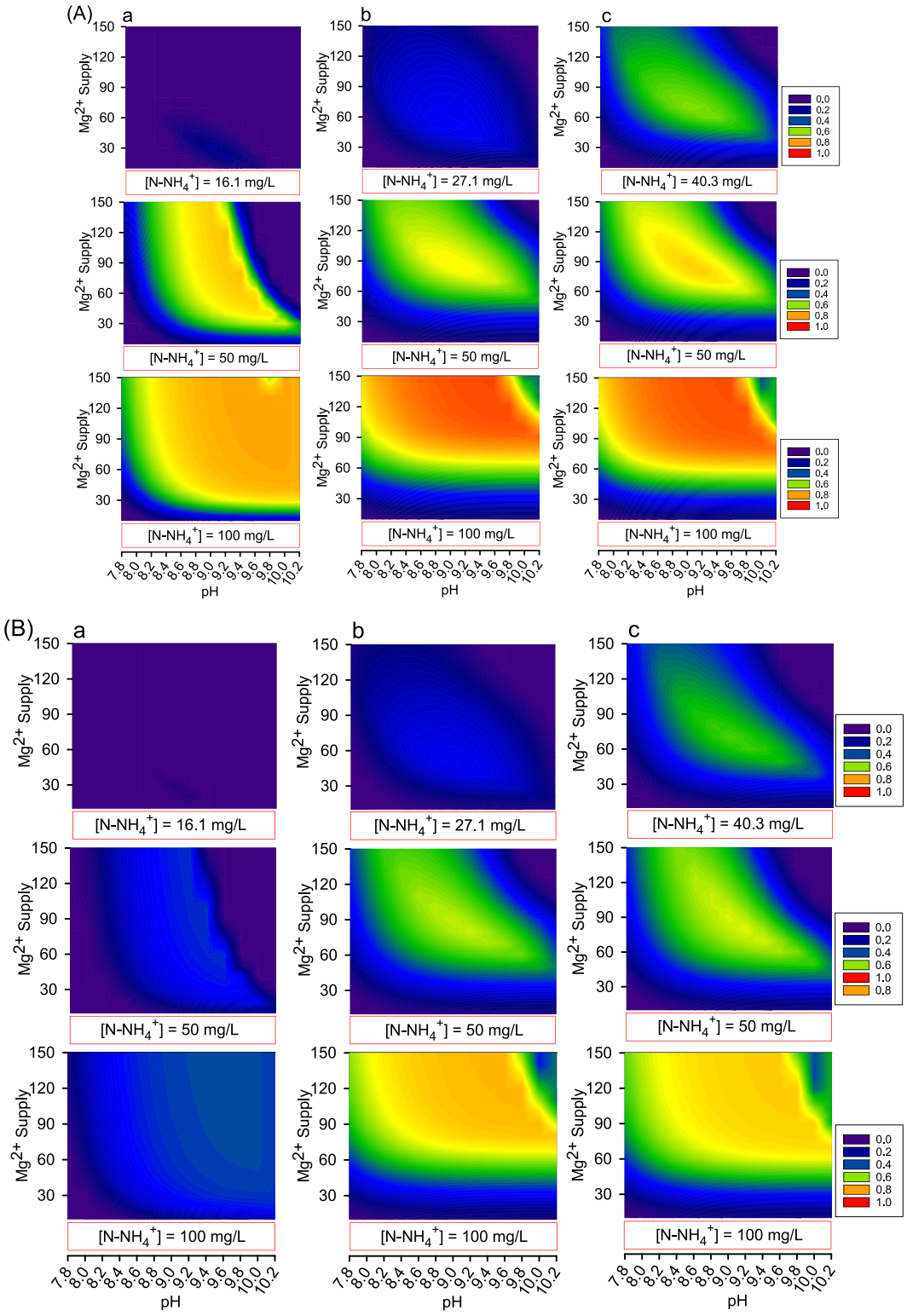

Fig. 6. The proportion of P-PO_4^{3-} precipitated as struvite under different Mg^{2+}, N-NH_4^+ and Ca^{2+} concentrations (A: 20 mgCa/L, B: 60 mgCa/L) for a: W1 - anaerobic WAS (7 L/d), b: W2 - fermented aerobic WAS (5 L/d) and c: W3 - fermented anaerobic WAS (7 L/d).

Table 5
Conditions for optimal P-recovery efficiency as struvite. Percentage refers to the maximum amount of P that could be recovered as precipitated struvite.

		$[Ca^{2+}]$ = 20 mg/L	$[Ca^{2+}]$ = 40 mg/L	$[Ca^{2+}]$ = 60 mg/L
		W1 – anaerobic WAS		
	pH	9.2	9.2	9.2
$[N\text{-}NH_4^+]$ = 16.1 mg/L	$Mg^{2+}/ P\text{-}PO_4^{3-}$	0.6:1	0.6:1	0.6:1
	Percentage	20.0 %	14.1 %	6.4 %
	pH	9.4	9.4	9.4
$[N\text{-}NH_4^+]$ = 50 mg/L	$Mg^{2+}/ P\text{-}PO_4^{3-}$	2.2:1	2.5:1	2.7:1
	Percentage	74.7 %	56.0 %	37.2 %
	pH	9.6	9.6	9.6
$[N\text{-}NH_4^+]$ = 75 mg/L	$Mg^{2+}/ P\text{-}PO_4^{3-}$	3:1	3:1	4:1
	Percentage	78.0 %	58.6 %	39.2 %
	pH	9.6	9.6	9.6
$[N\text{-}NH_4^+]$ = 100 mg/L	$Mg^{2+}/ P\text{-}PO_4^{3-}$	4:1	4:1	4:1
	Percentage	78.9 %	59.3 %	39.7 %
		W2 - Fermented aerobic WAS		
	pH	9	9.2	9.2
$[N\text{-}NH_4^+]$ = 27.1 mg/L	$Mg^{2+}/ P\text{-}PO_4^{3-}$	0.5:1	0.5:1	0.5:1
	Percentage	32.7 %	32.1 %	31.3 %
	pH	9.2	9.2	9.2
$[N\text{-}NH_4^+]$ = 50 mg/L	$Mg^{2+}/ P\text{-}PO_4^{3-}$	0.8:1	0.8:1	0.8:1
	Percentage	68.3 %	66.2 %	63.5 %
	pH	9.2	9.4	9.2
$[N\text{-}NH_4^+]$ = 75 mg/L	$Mg^{2+}/ P\text{-}PO_4^{3-}$	1.4:1	1.3:1	1.3:1
	Percentage	88.3 %	82.1 %	75.0 %
	pH	9.4	9.6	9.6
$[N\text{-}NH_4^+]$ = 100 mg/L	$Mg^{2+}/ P\text{-}PO_4^{3-}$	1.5:1	1.5:1	1.5:1
	Percentage	91.2 %	83.9 %	76.5 %
		W3 - Fermented anaerobic WAS		
	pH	9	9	9
$[N\text{-}NH_4^+]$ = 40.3 mg/L	$Mg^{2+}/ P\text{-}PO_4^{3-}$	0.8:1	0.8:1	0.8:1
	Percentage	59.0 %	57.1 %	54.7 %
	pH	9.2	9.2	9.2
$[N\text{-}NH_4^+]$ = 50 mg/L	$Mg^{2+}/ P\text{-}PO_4^{3-}$	1:1	1:1	1:1
	Percentage	73.4 %	69.9 %	65.0 %
	pH	9.4	9.4	9.4
$[N\text{-}NH_4^+]$ = 75 mg/L	$Mg^{2+}/ P\text{-}PO_4^{3-}$	1.4:1	1.4:1	1.5:1
	Percentage	88.5 %	80.7 %	72.5 %
	pH	9.6	9.6	9.6
$[N\text{-}NH_4^+]$ = 100 mg/L	$Mg^{2+}/ P\text{-}PO_4^{3-}$	1.8:1	1.8:1	1.8:1
	Percentage	90.3 %	81.9 %	73.5 %

percentage of struvite precipitation was only 24 % due to the lack of ammonium. $Mg_3(PO_4)_2$ was only precipitated for pH higher than 10.4. The proportion of $P\text{-}PO_4^{3-}$ precipitating as HAP was limited because the same amount of Ca^{2+} was considered while the $P\text{-}PO_4^{3-}$ concentration increased. Mg^{2+} and $N\text{-}NH_4^+$ played critical roles in the struvite precipitation process, which will be further explained with more detailed simulations in the next section.

3.4. Evaluation of magnesium requirements for P-recovery as struvite using visual MINTEQ

To comprehensively explore the struvite precipitation of the three scenarios, a pH range of 7.8 to 10.2 and different concentrations of Ca^{2+} were selected, and it was assumed that different levels of Mg^{2+} and $N\text{-}NH_4^+$ could be obtained by adding some external source of magnesium and ammonia nitrogen (Fig. 6). Stoichiometrically, 1 mol of struvite requires an equimolar ratio of $Mg^{2+}/ P\text{-}PO_4^{3-}/ N\text{-}NH_4^+$.

As expected, results in Fig. 6 show that the optimal molar ratio of $Mg^{2+}/ P\text{-}PO_4^{3-}$ for struvite formation varied according to pH. In general, more struvite was precipitated when the $N\text{-}NH_4^+$ content increased. Results for W2 show that the maximum proportion of total $P\text{-}PO_4^{3-}$ precipitated as struvite increased from 32.7 % to 91.2 % with the increase of $N\text{-}NH_4^+$ concentration from what was contented in the liquid phase of the fermentation process (27.1 mg/L) to 100 mg/L (as Fig. 6A-b shown). While W3 results show a similar trend but with maximum proportion from 59.0 % to 90.3 % (Fig. 6A-c). The difference appears from the higher $N\text{-}NH_4^+$ concentration (40.3 mg/L) and a slightly lower $P\text{-}PO_4^{3-}$ concentration in W3 vs W2. Case W1 was also in alignment with the other two cases about showing how $N\text{-}NH_4^+$ concentration is vital to struvite formation (Fig. 6A-a). At the same time, the limitation by Ca^{2+} precipitated as HAP competing $P\text{-}PO_4^{3-}$ with struvite became more visible in this scenario. Fig. 6B and Fig. S2 mainly show that the precipitated pH ranges of struvite generation were narrowed when the Ca^{2+} concentration increased from 20 to 60 mg/L. More intuitively, Fig. S3 shows the results of three scenarios of the specific $N\text{-}NH_4^+$ concentration (75 mg/L) with the increase of Ca^{2+} concentration. To sum up, it is essential to minimise the Ca^{2+} concentration and maximise the $N\text{-}NH_4^+$ concentration when aiming at recover $P\text{-}PO_4^{3-}$ as struvite.

Table 5 indicates the optimal conditions of pH and $Mg^{2+}/ P\text{-}PO_4^{3-}$ molar ratio for P-recovery as struvite under the three different scenarios. $N\text{-}NH_4^+$ concentration in W2 is lower than in the other scenarios since, under aerobic conditions, most of the ammonia has already been removed. Thus, less struvite is precipitated. At low $N\text{-}NH_4^+$ concentrations, Mg^{2+} would combine with $P\text{-}PO_4^{3-}$ to form $MgHPO_4{\cdot}3H_2O$ at pH lower than 8, and to form $Mg_3(PO_4)_2$ when the pH is above 8. On the contrary, with sufficient $N\text{-}NH_4^+$ content, this competition would be less relevant and the optimal $Mg^{2+}/ P\text{-}PO_4^{3-}$ molar ratio would remain at 1.5 (90 % of P as struvite with 20 mg Ca^{2+}/L). Despite the fact that the results of the two scenarios for anaerobic WAS showed similar trends, W1 needed a higher $Mg^{2+}/ P\text{-}PO_4^{3-}$ molar ratio (i.e. 4) to have 78 % of P precipitated as struvite. However, this proportion can be increased up to 90 % of P in W3 with a $Mg^{2+}/ P\text{-}PO_4^{3-}$ molar ratio of 1.8. The higher the $P\text{-}PO_4^{3-}$ concentration, the less the Mg^{2+} amount required to precipitate as much as P as possible as struvite.

Considering the best precipitation conditions for each case, the percentage of P that could be recovered with respect to the P load to the

plant can be calculated (Table 4). For case W1, 19.2 % of total P could be recovered as struvite while up to 24 % could be recovered as precipitated P. These percentages are increased after fermentation. For the case W2, 38.1 % could be recovered as struvite and up to 41.2 % as total P precipitate. Finally, the best P-recovery is predicted for case W3, where these percentages increased to 46.6 % recovered as struvite and up to 51 % recovered as precipitate.

Finally, it must be assumed that a scenario-specific study for a given wastewater and WWTP would be necessary to obtain an accurate description of the expected results. For example, the carbonate content in the wastewater can modify the specific results, as it is involved in the N-P-Mg-Ca equilibria. When a high amount of carbonate is present, Mg^{2+} will first combine with carbonate to form magnesite, leading to more dissolved phosphate. In this case, the same P-recovery efficiency could be obtained, but at the cost of requiring a higher Mg^{2+} addition.

3.5. Practical implications

The results reported in this work represent the maximum amount of P-recovery achievable from these specific streams assuming ideal operation of all treatment steps. For instance, an optimal pH setpoint is fixed using a pH control loop able to maintain pH at this setpoint even under variable operation and/or disturbances. Moreover, we considered a well-designed precipitation reactor allowing to reach the ideal thermodynamic limits for precipitation. We also assumed that the supernatant liquid phase could be completely separated from the biomass. Consequently, lower P-recovery is to be expected in a full-scale WWTP when any of these assumptions is not met.

In any case, the comparison of the three scenarios for P-recovery from an A_2O WWTP clearly indicates that the best option for P-recovery would be the use of the supernatant from the anaerobic fermentation of WAS, where up to 51 % of P-recovery could be achieved. The rest of the P is in the sludge and, thus, global P-recovery could be improved by treating the biomass stream with some additional specific treatment for P release.

Finally, this study only focuses on the amount of P-recovery that could be obtained in this A_2O configuration. A comprehensive economic evaluation is required to assess its feasibility since investment in additional units such as a reactor for anaerobic fermentation of biomass and separation of the liquid stream would be necessary. Furthermore, the cost of chemical reagents such as magnesium salts and acid/base for pH control, even if obtained from subproducts, should be offset by the benefits obtained from the struvite revenues and by the decrease in maintenance costs due to the reduction of undesired struvite precipitation.

4. Conclusions

This work investigated the P-recovery potential of different WAS extraction strategies in a continuous A_2O system with stable EBPR performance. The main conclusions are:

- Successful P and COD removal can be obtained independently of the aerobic or anaerobic WAS extraction. Full COD and ammonium removal could also be reached under all conditions. Purging from the anaerobic reactor improved PAO activity, increasing anaerobic P concentration by 27 %. Up to 24 % of the input P could be extracted within the supernatant of the anaerobic WAS extraction.
- WAS fermentation tests showed that the anaerobic WAS only took 3 days to release a high amount of P while 7 days were required for the aerobic WAS. The maximum P-recovery from the supernatant could be increased up to 51.6 % for the anaerobic fermented WAS.
- Simulation results showed that a pH range from 8 to 10.6 was required for struvite precipitation. However, the limitation by magnesium and ammonium in the WAS streams only allowed a maximum struvite precipitation of 24 % for the fermented anaerobic WAS and 32 % for the fermented aerobic WAS.
- The study of different scenarios with Mg^{2+} and $N\text{-}NH_4^+$ addition showed that a maximum P-recovery as precipitated P could be 51 % in the scenario with fermented anaerobic WAS. The concentrations of Ca^{2+} and $N\text{-}NH_4^+$ are key to have a precipitate with high percentage of struvite due to the competition with other species such as HAP, $MgHPO_4{\cdot}3H_2O$ and $Mg_3(PO_4)_2$.

CRediT authorship contribution statement

Mengqi Cheng: Data curation, Formal analysis, Methodology, Writing – original draft. **Congcong Zhang:** Data curation, Formal analysis, Methodology, Writing – original draft. **Albert Guisasola:** Conceptualization, Data curation, Funding acquisition, Supervision, Visualization, Writing – review & editing. **Juan Antonio Baeza:** Conceptualization, Data curation, Funding acquisition, Methodology, Supervision, Visualization, Writing – review & editing.

Declaration of competing interest

The authors declare that they have no known competing financial interests or personal relationships that could have appeared to influence the work reported in this paper.

Data availability

Data will be made available on request.

Acknowledgements

This work was supported by Grant PID2020-119018RB-I00 funded by MCIN/AEI/10.13039/501100011033 and by European Union NextGenerationEU/PRTR. Congcong Zhang and Mengqi Cheng would like to thank the financial support from China Scholarship Council (nums 201806330084 and 202108310149, respectively) . The authors are members of the GENOCOV research group (Grup de Recerca Consolidat de la Generalitat de Catalunya, 2021 SGR 515, www.genocov.com).

Appendix A. Supplementary data

Supplementary data to this article can be found online at https://doi.org/10.1016/j.scitotenv.2023.168898.

References

Annisa, T., Azkiya, A., Fauzi, R., N., B D Nandiyanto, A., Hofifah, S.N., 2021. Cost analysis and economic evaluation for manufacturing hydroxyapatite nanoparticles from eggshell waste. Int. J. Res. Appl. Technol. 1, 211–226. https://doi.org/10.34010/injuratech.v1i1.5669.

Baeza, J.A., 2022. Advanced direct digital control (AddControl): Lessons learned from 20 years of adding control to lab and pilot scale treatment systems, In: 13th IWA Conference on Instrumentation, Control and Automation. ICA 2022. Tsinghua University, Beijing (China), pp. 13–15.

Baeza, J.A., Guerrero, J., Guisasola, A., 2017. Optimising a novel SBR configuration for enhanced biological phosphorus removal and recovery (EBPR2). Desalination Water Treat 68, 319–329. https://doi.org/10.5004/dwt.2017.20468.

Bouzas, A., Martí, N., Grau, S., Barat, R., Mangin, D., Pastor, L., 2019. Implementation of a global P-recovery system in urban wastewater treatment plants. J. Clean. Prod. 227, 130–140. https://doi.org/10.1016/j.jclepro.2019.04.126.

Broughton, A., Pratt, S., Shilton, A., 2008. Enhanced biological phosphorus removal for high-strength wastewater with a low rbCOD:P ratio. Bioresour. Technol. 99, 1236–1241. https://doi.org/10.1016/j.biortech.2007.02.013.

Cornel, P., Schaum, C., 2009. Phosphorus recovery from wastewater: needs, technologies and costs. Water Sci. Technol. 59, 1069–1076. https://doi.org/10.2166/wst.2009.045.

Egle, L., Rechberger, H., Krampe, J., Zessner, M., 2016. Phosphorus recovery from municipal wastewater: an integrated comparative technological, environmental and economic assessment of P recovery technologies. Sci. Total Environ. 571, 522–542. https://doi.org/10.1016/j.scitotenv.2016.07.019.

Elduayen-Echave, B., Lizarralde, I., Larraona, G.S., Ayesa, E., Grau, P., 2019. A new mass-based discretized population balance model for precipitation processes:

application to struvite precipitation. Water Res. 155, 26–41. https://doi.org/10.1016/j.watres.2019.01.047.
European Commission, 2017. Communication from the Commission: On the 2017 List of Critical Raw Materials for the EU. European Commission: Brussels, Belgium COM no. 490.
Forrest, A.L., Fattah, K.P., Mavinic, D.S., Koch, F.A., 2008. Optimizing struvite production for phosphate recovery in WWTP. J. Environ. Eng. 134, 395–402. https://doi.org/10.1061/(ASCE)0733-9372(2008)134:5(395).
Guisasola, A., Chan, C., Larriba, O., Lippo, D., Suárez-Ojeda, M.E., Baeza, J.A., 2019. Long-term stability of an enhanced biological phosphorus removal system in a phosphorus recovery scenario. J. Clean. Prod. 214, 308–318. https://doi.org/10.1016/j.jclepro.2018.12.220.
Gustafsson, J.P., 2005. Visual MINTEQ 3.1 user guide.
Hermassi, M., Valderrama, C., Dosta, J., Cortina, J.L., Batis, N.H., 2015. Evaluation of hydroxyapatite crystallization in a batch reactor for the valorization of alkaline phosphate concentrates from wastewater treatment plants using calcium chloride. Chem. Eng. J. 267, 142–152. https://doi.org/10.1016/j.cej.2014.12.079.
Hutnik, N., Piotrowski, K., Wierzbowska, B., Matynia, A., 2011. Continuous reaction crystallization of struvite from phosphate(V) solutions containing calcium ions. Cryst. Res. Technol. 46, 443–449. https://doi.org/10.1002/crat.201100049.
Larriba, O., Rovira-Cal, E., Juznic-Zonta, Z., Guisasola, A., Baeza, J.A., 2020. Evaluation of the integration of P recovery, polyhydroxyalkanoate production and short cut nitrogen removal in a mainstream wastewater treatment process. Water Res. 172, 115474 https://doi.org/10.1016/j.watres.2020.115474.
Lee, S.-H., Yoo, B.-H., Lim, S.J., Kim, T.-H., Kim, S.-K., Kim, J.Y., 2013. Development and validation of an equilibrium model for struvite formation with calcium co-precipitation. J. Cryst. Growth 372, 129–137. https://doi.org/10.1016/j.jcrysgro.2013.03.010.
Li, B., Boiarkina, I., Young, B., Yu, W., 2016. Quantification and mitigation of the negative impact of calcium on struvite purity. Adv. Powder Technol. 27, 2354–2362. https://doi.org/10.1016/j.apt.2016.10.003.
Metcalf&Eddy, George, T., H.David, S., Ryujiro, T., Franklin .B., L, Mohammad, A.-O., Gregory, B., Willian, P., 2014. Wastewater Engineering: Treatment and Resource Recovery, 5th, edition. ed. McGraw-Hill Education New York, Newyork.
Natividad-Marin, L., Burns, M.W., Schneider, P., 2023. A comparison of struvite precipitation thermodynamics and kinetics modelling techniques. Water Sci. Technol. 87, 1393–1422. https://doi.org/10.2166/wst.2023.061.
Rey-Martínez, N., Guisasola, A., Baeza, J.A., 2022. Assessment of the significance of heavy metals, pesticides and other contaminants in recovered products from water resource recovery facilities. Resour. Conserv. Recycl. 182, 106313 https://doi.org/10.1016/j.resconrec.2022.106313.
Sarria, N.V., Rivera Velasco, D.M., Larrahondo Chávez, D.A., Mazuera Ríos, H.D., Gandini Ayerbe, M.A., Goyes López, C.E., Mejía Villareal, I.M., 2022. Struvite and hydroxyapatite recovery from wastewater treatment plant at Autónoma de Occidente University, Colombia. Case Studies in Chemical and Environmental Engineering 6, 100213. https://doi.org/10.1016/j.cscee.2022.100213.
Sena, M., Seib, M., Noguera, D.R., Hicks, A., 2021. Environmental impacts of phosphorus recovery through struvite precipitation in wastewater treatment. J. Clean. Prod. 280, 124222 https://doi.org/10.1016/j.jclepro.2020.124222.
Shih, K., Yan, H., 2016. The crystallization of struvite and its analog (K-Struvite) from waste streams for nutrient recycling. Environmental Materials and Waste: Resource Recovery and Pollution Prevention 665–686. https://doi.org/10.1016/B978-0-12-803837-6.00026-3.
Venkiteshwaran, K., McNamara, P.J., Mayer, B.K., 2018. Meta-analysis of non-reactive phosphorus in water, wastewater, and sludge, and strategies to convert it for enhanced phosphorus removal and recovery. Sci. Total Environ. 644, 661–674. https://doi.org/10.1016/j.scitotenv.2018.06.369.
Zhang, C., Guisasola, A., Baeza, J.A., 2022. A review on the integration of mainstream P-recovery strategies with enhanced biological phosphorus removal. Water Res. 212, 118102 https://doi.org/10.1016/j.watres.2022.118102.
Zhang, C., Guisasola, A., Oehmen, A., Baeza, J.A., 2023. Benefits and drawbacks of integrating a side-stream sludge fermenter into an A2O system under limited COD conditions. Chem. Eng. J. 468, 143700 https://doi.org/10.1016/j.cej.2023.143700.